JBC RESEARCH ARTICLE

RGS4 controls airway hyperresponsiveness through GAP-independent mechanisms

Received for publication, August 24, 2023, and in revised form, February 12, 2024 Published, Papers in Press, March 2, 2024,
https://doi.org/10.1016/j.jbc.2024.107127

Ilin V. Joshi[1], **Eunice C. Chan**[1], **Justin B. Lack**[2], **Chengyu Liu**[3], **and Kirk M. Druey**[1,*]

From the [1]*Lung and Vascular Inflammation Section, Laboratory of Allergic Diseases, National Institute of Allergy and Infectious Diseases, National Institutes of Health, Bethesda, Maryland, USA;* [2]*NIAID Collaborative Bioinformatics Resource, National Institute of Allergy and Infectious Diseases, National Institutes of Health, Bethesda, Maryland, USA;* [3]*Transgenic Core, NHLBI/NIH, Bethesda, Maryland, USA*

Reviewed by members of the JBC Editorial Board. Edited by Henrik Dohlman

Regulators of G protein signaling (RGS) proteins constrain G protein-coupled receptor (GPCR)–mediated and other responses throughout the body primarily, but not exclusively, through their GTPase-activating protein activity. Asthma is a highly prevalent condition characterized by airway hyper-responsiveness (AHR) to environmental stimuli resulting in part from amplified GPCR-mediated airway smooth muscle contraction. *Rgs2* or *Rgs5* gene deletion in mice enhances AHR and airway smooth muscle contraction, whereas RGS4 KO mice unexpectedly have decreased AHR because of increased production of the bronchodilator prostaglandin E2 (PGE2) by lung epithelial cells. Here, we found that knockin mice harboring *Rgs4* alleles encoding a point mutation (N128A) that sharply curtails RGS4 GTPase-activating protein activity had increased AHR, reduced airway PGE2 levels, and augmented GPCR-induced bronchoconstriction compared with either RGS4 KO mice or WT controls. RGS4 interacted with the p85α subunit of PI3K and inhibited PI3K-dependent PGE2 secretion elicited by transforming growth factor beta in airway epithelial cells. Together, these findings suggest that RGS4 affects asthma severity in part by regulating the airway inflammatory milieu in a G protein-independent manner.

Patients with asthma experience wheezing, cough, and shortness of breath resulting from intermittent and reversible airway obstruction (1). In more than half of the cases, environmental allergen exposure induces a specific immunoglobulin E antibody response, activation of lung-resident cells, including epithelial cells, mast cells, and innate lymphoid type 2 cells, production of type 2 cytokines (*e.g.*, interleukin [IL]-4, 5, 13), and infiltration of type 2 $CD4^+$ T lymphocytes and eosinophils (2). This leads to chronic airway inflammation and lung tissue remodeling, which contribute to the development of airway hyper-responsiveness (AHR) (3).

G protein-coupled receptors (GPCRs) mediate several aspects of the asthma phenotype. Muscarinic acetylcholine (ACh) receptors in the airways induce airway smooth muscle (ASM) contraction, whereas chemokine receptors mediate leukocyte trafficking to and within inflamed lung tissue (4). We and others have investigated the role of regulator of G protein signaling (RGS) proteins expressed in lung to control these and other processes. Within the lung compartment, RGS2 and 4 are expressed in airway epithelial cells (AECs) and ASMs, whereas RGS5 expression is limited to ASM (5–8). RGS4 expression in human bronchial epithelium increases with asthma severity, and our experimental findings support the hypothesis that RGS4 promotes AHR by suppressing prostaglandin E2 (PGE2) biosynthesis in the human respiratory epithelium (7). Although RGS4 inhibits protease-activated receptor 2–mediated PGE2 secretion by AECs *in vitro*, the importance of this or other pathways involved in PGE2 production in the airways remains unknown.

All RGS proteins contain a signature RGS domain that in most but not all cases confers GTPase-activating protein (GAP) activity on alpha subunits of the heterotrimeric G protein complex, which is thought to reduce the pool of activated (GTP-bound) Gα and thereby limit GPCR activation (9, 10). There are four RGS subfamilies based on sequence homology (A/RZ, B/R4, C/R7, and D/R12). Several of the larger RGS proteins contain additional domains that mediate scaffolding functions. RGS14 (in the R12 family) binds diverse intracellular signaling proteins including Ras and Rap monomeric G proteins, CaM-dependent kinase II, and Raf kinase (11). Although RGS4, which is a member of the R4 subfamily, does not contain known additional protein-binding domains, it has documented interactions with several proteins other than Gα including calmodulin (12), ErbB3 receptors (13), and the vesicle protein β′-COP (14). Previously, we found that several R4 RGS proteins including RGS4 associate with the regulatory p85α subunit of PI3K only in its phosphorylated state and constrain PI3K-mediated signaling by interfering with its binding to receptors (15, 16). In human ASM cells, RGS4 coimmunoprecipitates with p85α and controls proliferation induced by platelet-derived growth factor (17). Here, we set out to determine the relative importance of RGS4 GAP-mediated and GAP-independent functions for AHR in an experimental model of asthma.

Results

Characterization of RGS4 mutant mice

To determine the role of RGS4 GAP activity in AHR, we focused on a highly conserved asparagine residue (N128A in

* For correspondence: Kirk M. Druey, kdruey@niaid.nih.gov.

RGS4) present in all R4, R7, and R12 RGS proteins (Fig. 1*A*) (18, 19). Mutation of this residue nearly abolishes RGS4 and related R4 RGS protein GAP activity on Gαi/o *in vitro* (18, 20). To create a suitable animal model for these studies, we applied CRISPR–Cas9 technology by microinjecting a single guide RNA (sgRNA), oligonucleotide donor, and Cas9 mRNA into mouse zygotes to establish lines harboring alleles encoding RGS4(N128A) (subsequently referred to as "NA" mice) (Fig. S1). Sanger resequencing of genomic DNA confirmed germline transmission of the mutation (Fig. 1*B*). These mice developed normally and were born at the expected Mendelian frequencies. *Rgs4* transcript abundance in several organs from NA mice, including those with the highest RGS4 expression, such as heart, lung, and brain, was similar to that in WT controls (Fig. 1*C*). RGS4 protein expression in brain tissue detected by immunoblotting was similar in tissue from WT and NA mice (Fig. 1, *D* and *E*). Within the lung tissue, *Rgs2* expression in NA mice was equivalent to that seen in WT or RGS4 KO mice, whereas *Rgs5* expression was significantly lower in lungs from NA mice than in WT controls (Fig. 1*F*). Fluorescence microscopy of GFP-RGS4 expressed in human embryonic kidney 293T (HEK293T) cells revealed similar diffuse cytosolic localization of either the WT or N128A variant RGS4 proteins (Fig. 1*G*).

Homozygous RGS4 NA mice exhibited no gross phenotypic abnormalities and had normal body weights. Histological analysis of major organs, including brain, heart, and lung, revealed no obvious abnormalities (Fig. 2*A*). However, like RGS4 KO mice (21), liver sections from NA mice were vacuolated, suggestive of parenchymal lipid deposits and hepatic steatosis (Fig. 2*B*). Blood examination revealed that levels of hemoglobin and various leukocyte numbers were similar in NA mice and WT controls, indicating normal hematopoiesis (Fig. 2, *C–E*).

AHR in RGS4(N128A) mice

To examine AHR in an experimental model of asthma, we sensitized and challenged mice with extracts of *Aspergillus fumigatus* (*Af*), a ubiquitous allergenic mold associated with severe asthma (22), and measured airway resistance in live mice by plethysmography. Total lung resistance was significantly higher in NA mice than in RGS4 KO mice or WT controls (Fig. 3*A*) after challenge with various doses of the bronchoconstrictor methacholine (MCh, an ACh analog). Consistent with our previous studies (7), Newtonian resistance (R_n), which primarily reflects contraction of the larger and smooth muscle–layered airways not involved in gas exchange (23), was markedly lower in *Af*-challenged RGS4 KO mice than in NA mice or WT controls (Fig. 3*B*).

Collectively, these findings suggested that RGS4 exerts complex control over lung physiology through both GAP-dependent and GAP-independent mechanisms. To delineate the pathways involved, we first examined allergic airway inflammation. Neither total leukocyte counts nor leukocyte composition of bronchoalveolar lavage fluid (BALF) (*e.g.*, percentage of eosinophils) differed significantly in NA and WT

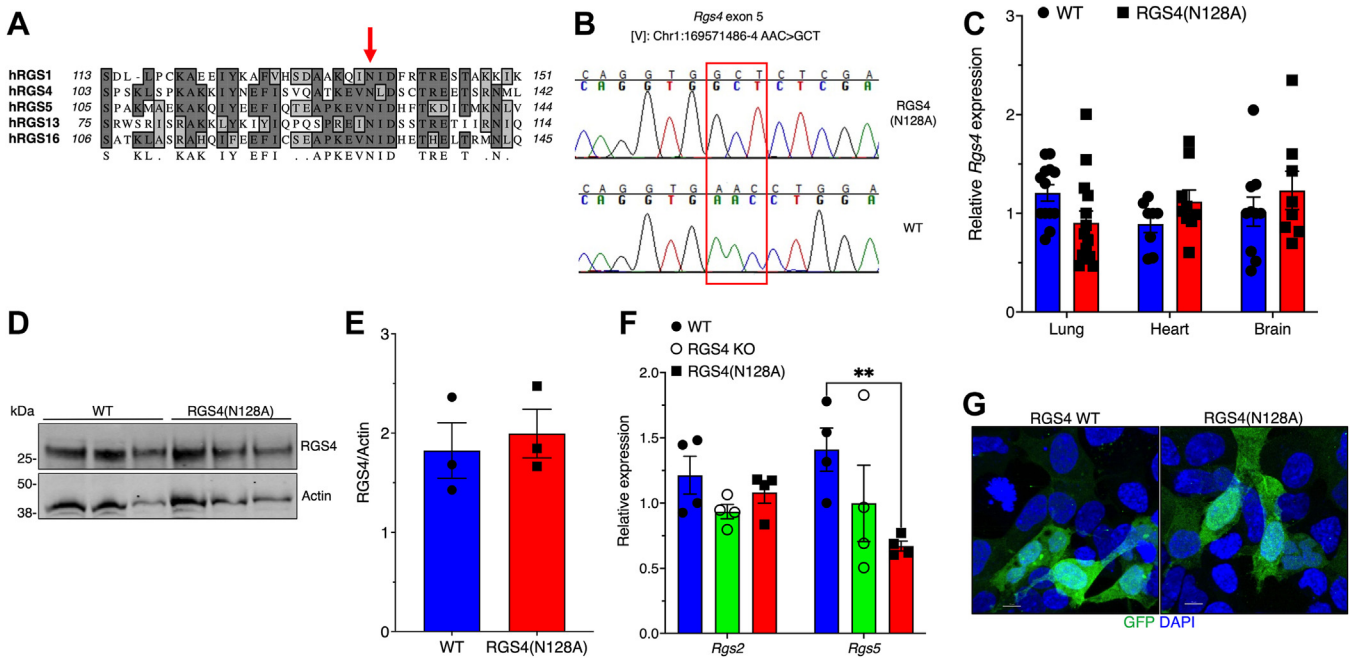

Figure 1. Generation of RGS4(N128A) mice. *A*, alignment of several R4 RGS proteins. *Arrow* indicates the highly conserved Asn residue located in the RGS domain that is critical for GAP activity. *B*, chromatographs of the N128A mutation from sequencing of genomic DNA from homozygous RGS4(N128A) or WT mice; chromosomal coordinates (GRCm39) are indicated above. *C*, *Rgs4* expression in various tissues determined by quantitative PCR. Means ± SEM from n = 8 to 14 mice/group. *D* and *E*, RGS4 expression in brain tissue determined by IP/WB; representative blot (*D*); quantification of RGS4/actin (*E*); means ± SEM from n = 3 mice/group. *F*, *Rgs2* and *Rgs5* expression in lung tissue determined by quantitative PCR. Means ± SEM from n = 4 mice/group; $^{**}p = 0.009$, two-way ANOVA test, Tukey's multiple comparisons test. *G*, fluorescence microscopy images of GFP-RGS4 (WT or N128A) in transfected HEK293T cells. Scale bar represents 10 μm. GAP, GTPase-activating protein; HEK293T, human embryonic kidney 293T cell line; IP, immunoprecipitation; RGS, regulator of G protein signaling; WB, Western blot.

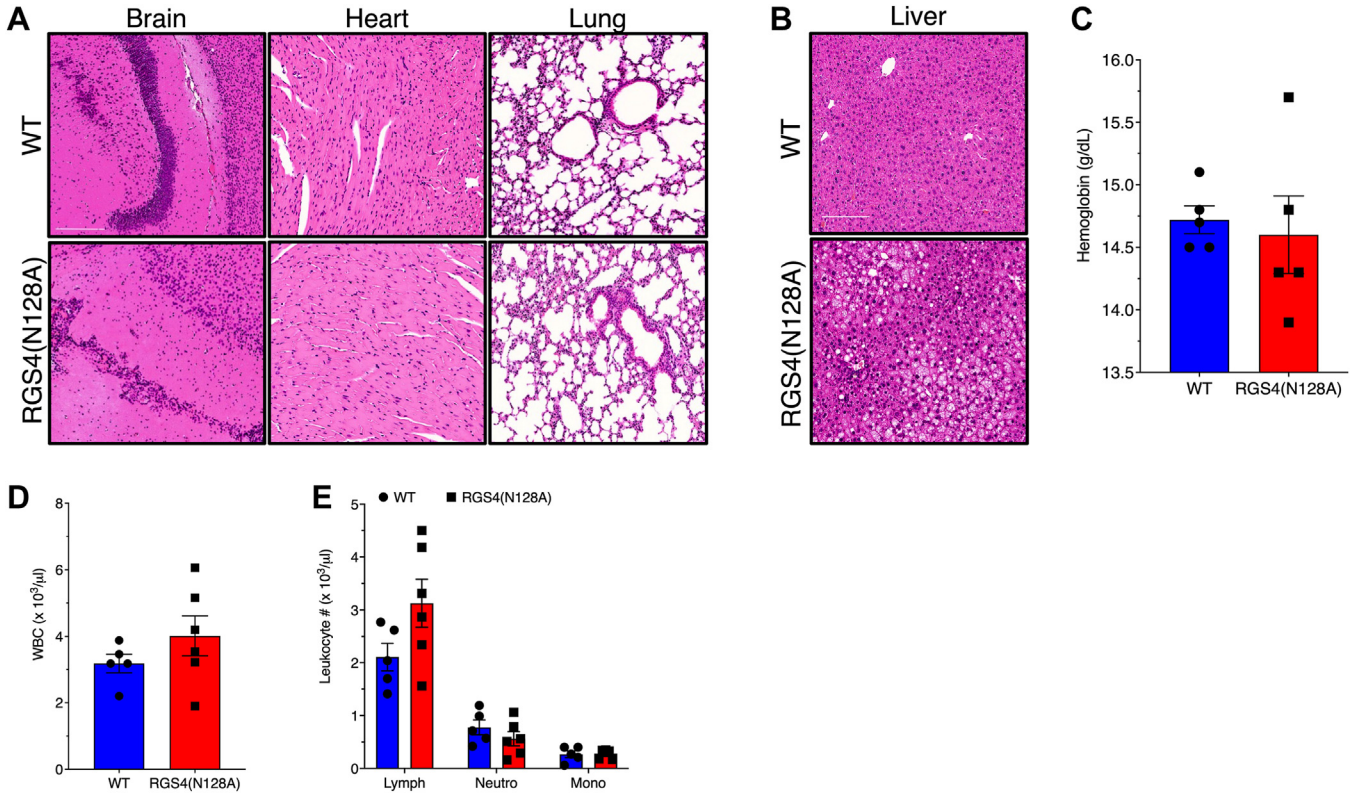

Figure 2. NA mice exhibit fatty liver at homeostasis. *A* and *B*, histology of brain, heart, lung, and liver (*B*) from WT and NA mice detected by H&E staining. Images representative of n = 3 mice/group. Scale bar represents 250 µm. *C–E*, blood examination from WT and NA mice including hemoglobin (*C*), total white blood cells (*D*), and differential leukocyte counts (*E*); means ± SEM from n = 5 to 6 mice/group.

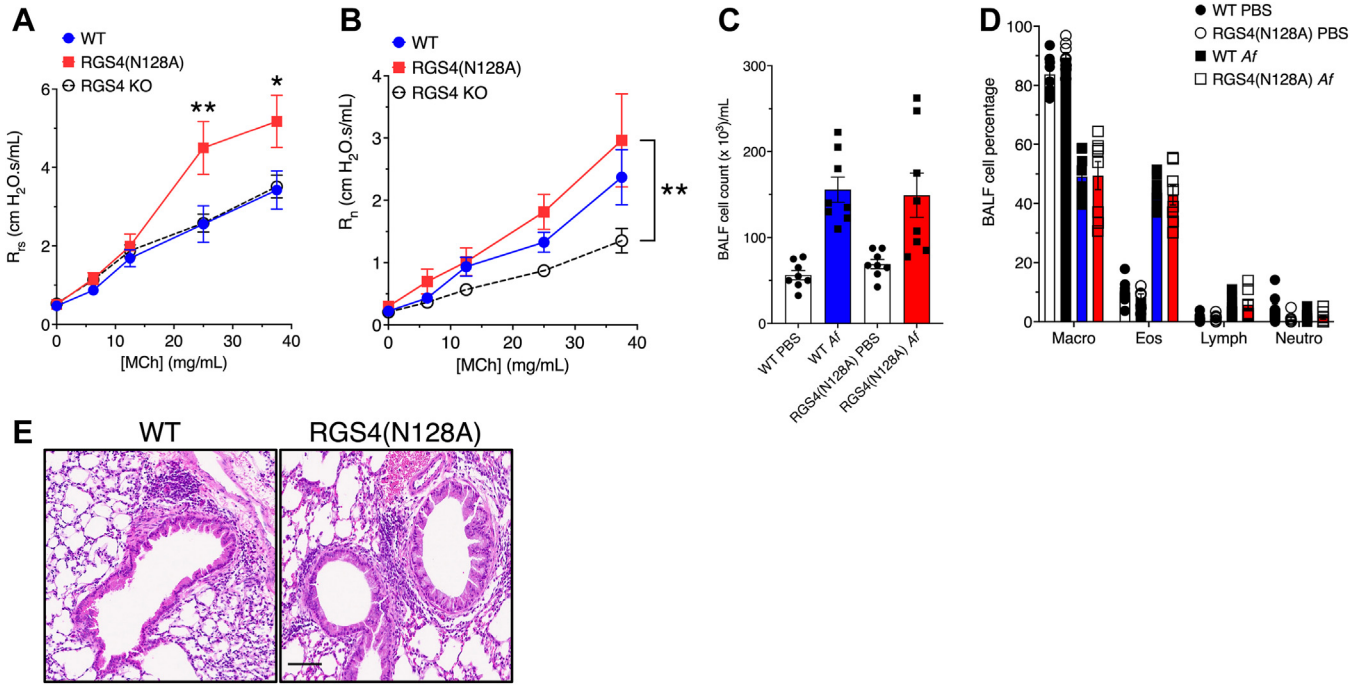

Figure 3. RGS4(N128A) mice have increased AHR in an experimental model of asthma. *A* and *B*, lung resistance (R_{rs}, *A* or R_n, *B*) in live *Af*-challenged mice determined by plethysmography. Means ± SEM from n = 4 to 8 mice/group, $^{**}p < 0.004$, $^{***}p = 0.0002$, WT *versus* NA, two-way ANOVA test, Tukey's multiple comparisons test. *C* and *D*, BALF total leukocyte counts (*C*) and composition (*D*) from PBS (naïve) or *Af*-challenged WT or NA mice. Means ± SEM from eight mice/group. *E*, H&E-stained lung sections from WT or NA mice. Images representative of four mice/group. Scale bar represents 100 µm. *Af*, *Aspergillus fumigatus*, AHR, airway hyper-responsiveness; BALF, bronchoalveolar lavage; RGS, regulator of G protein signaling.

controls (Fig. 3, *C* and *D*). Histological examination of lung sections demonstrated comparable inflammation (peribronchial "cuffing" predominantly with eosinophils) in WT and NA mice (Fig. 3*E*).

Levels of asthma-associated cytokines in BALF including IL-1β, IL-4, 5, 10, 13, 17, and eotaxin were also comparable in *Af*-challenged NA and WT mice but were significantly lower than in RGS4 KO mice (Figs. 4, *A–D* and S2, *A–C*). Allergic proinflammatory mediators including IL-13 induce goblet cell hyperplasia in the respiratory epithelium, increased mucin expression, and mucous secretion into the lumen, which also contribute to increased airway resistance (24). The bronchial epithelium of RGS4 NA mice had significantly more mucin expression than WT controls, as indicated by periodic acid Schiff (PAS) staining (Fig. 4, *E* and *F*). Thus, while RGS4 GAP activity is not critical for regulation of cytokine production in the airways, it may inhibit G protein-mediated mucin expression within the respiratory epithelium.

RGS4 inhibits airway contraction through its GAP activity

Chronic inflammation and airway remodeling increase airway luminal resistance through several mechanisms including ASM hyperproliferation, increased deposition of extracellular matrix components, and mucous plugging (25). To determine the effect of the N128A mutation on ASM contractility, we examined airway mechanics in naïve mice. Both R_n and R_{rs} were significantly higher in naïve NA mice than in WT or RGS4 KO mice after exposure to MCh (Fig. 5, *A* and *B*), suggesting ASM hypercontraction. To visualize ASM contraction directly, we quantified airway diameter in precision cut lung slices (PCLSs) from naïve mice *ex vivo* in response to stimulation with various concentrations of carbachol (CCh, an ACh analog). CCh-treated airways from NA mice contracted significantly more than those from either WT or RGS4 KO mice (Fig. 5, *C* and *D*). Consistent with our previous studies, contraction of PCLS from RGS4 KO mice did not differ from WT (7). Collectively, these results suggested that RGS4 inhibits cholinergic-dependent airway contraction through its GAP activity.

RGS4 suppresses GPCR-independent PGE2 production in lung

Previously, we determined that RGS4 KO mice had less AHR because of increased airway PGE2 levels (7). Unexpectedly, PGE2 levels in BALF from *Af*-challenged NA mice were significantly lower than that from either WT controls or RGS4 KO mice (Fig. 6*A*). This result suggested that RGS4 may inhibit airway PGE2 biosynthesis independently of its GAP activity. Given the interaction of RGS4 with p85α, we

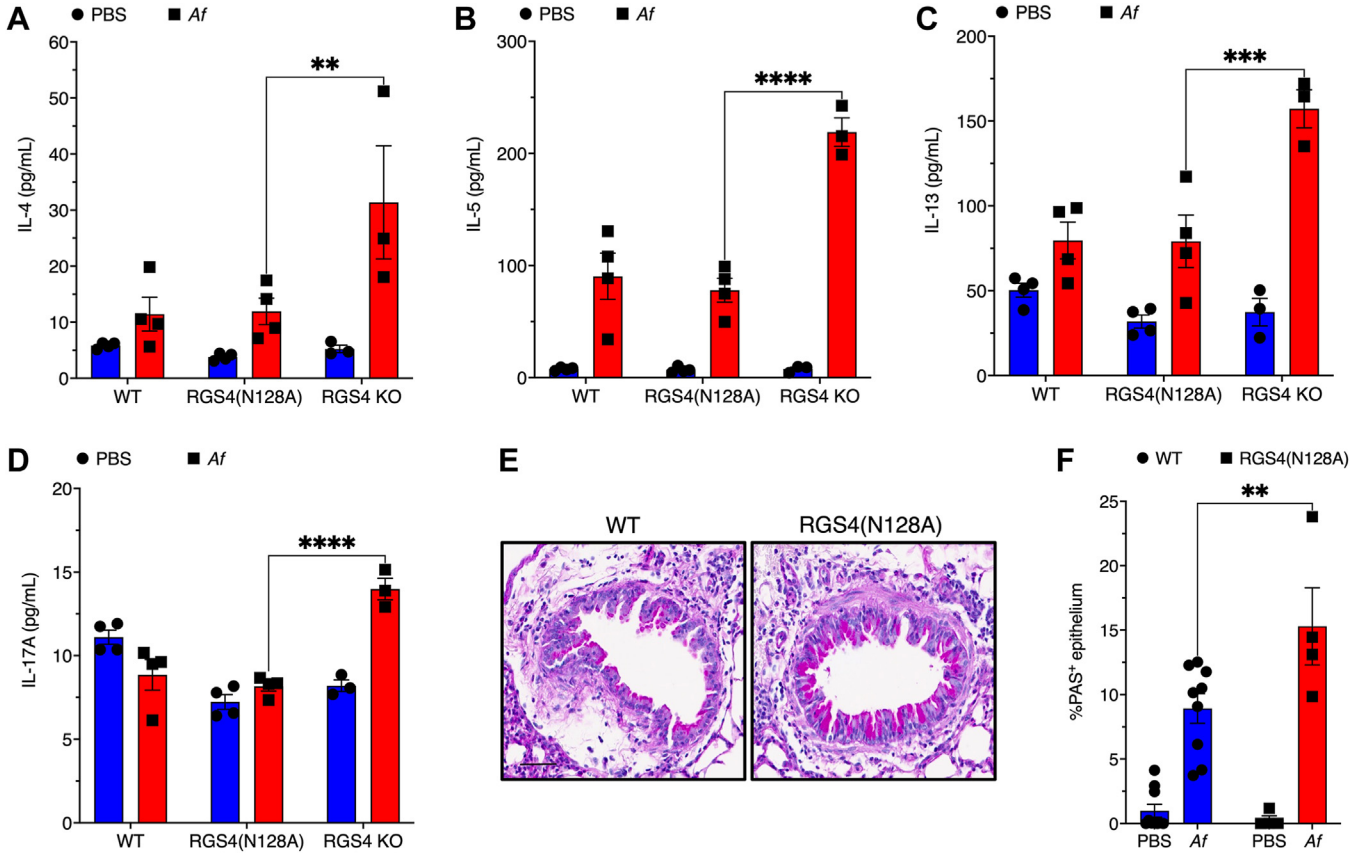

Figure 4. Airway inflammatory milieu in RGS4(N128A) mice. *A–D*, allergy-associated cytokines IL-4 (*A*), IL-5 (*B*), IL-13 (*C*), and IL-17A (*D*) in BALF. Means ± SEM from four mice/group, $^{**}p = 0.006$, $^{***}p = 0.0002$, $^{****}p < 0.0001$, two-way ANOVA test, Tukey's multiple comparisons test. *E*, periodic acid Schiff (PAS)–stained lung sections from *Af*-challenged mice. Scale bar represents 100 μm. *F*, quantification of airway PAS staining; means ± SEM from $n = 4$ to 9 mice/group. $^{**}p = 0.005$, two-way ANOVA test, Sidak's multiple comparisons test. *Af*, *Aspergillus fumigatus*; BALF, bronchoalveolar lavage; IL, interleukin; RGS, regulator of G protein signaling.

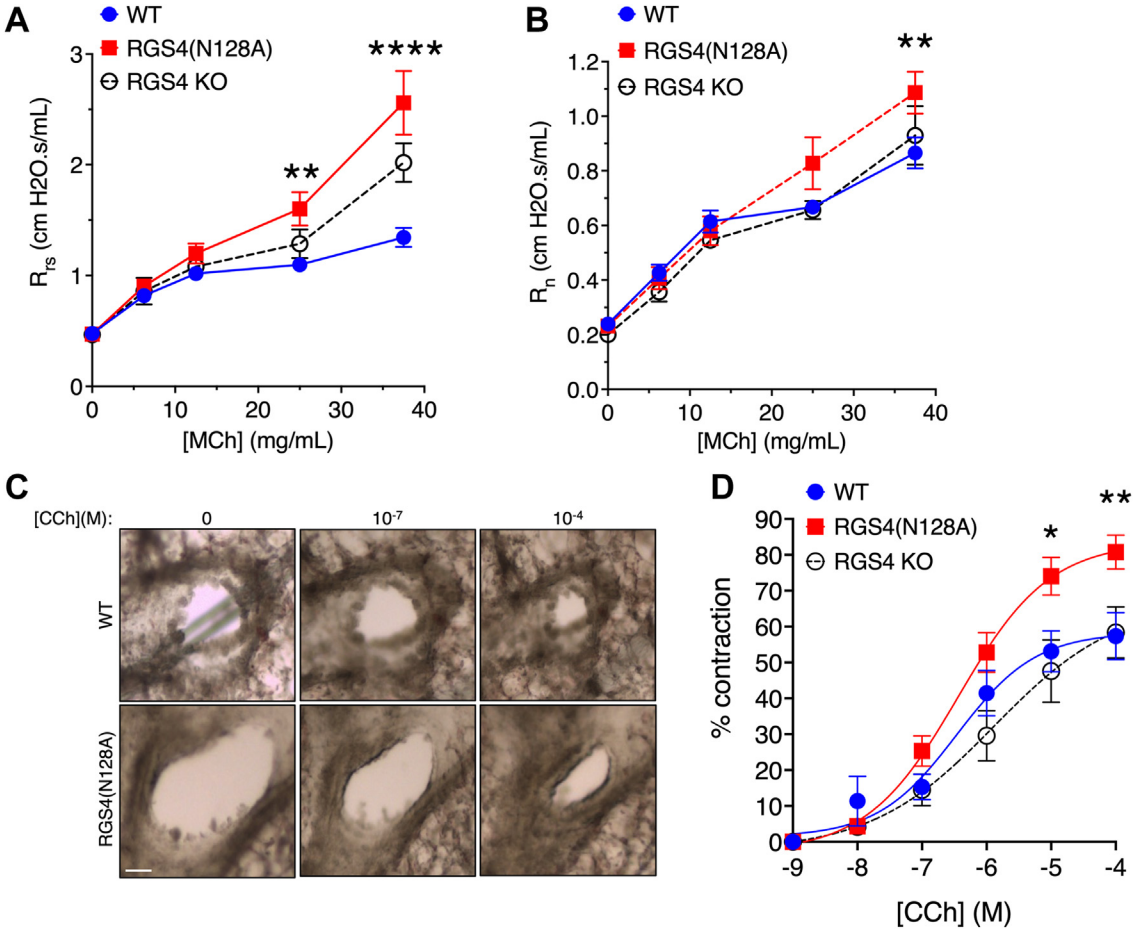

Figure 5. Airway mechanics in RGS4(N128A) mice. *A* and *B*, lung resistance (R_{rs}, *A*) or (R_n, *B*) in naïve (PBS challenged) mice. n = 4 to 8 mice/group. $^{**}p < 0.008$, $^{****}p < 0.0001$, NA mice *versus* WT, two-way ANOVA test, Tukey's multiple comparisons test. *C* and *D*, representative images of airway contraction in PCLS stimulated with CCh (*C*) and quantified (*D*). Means ± SEM from n = 2 mice/group (8–16 airways); $^{*}p = 0.01$, $^{**}p = 0.004$, NA mice *versus* WT, two-way ANOVA test, Tukey's multiple comparisons test. Scale bar represents 100 μm. CCh, carbachol; PCLS, precision cut lung slice; RGS, regulator of G protein signaling.

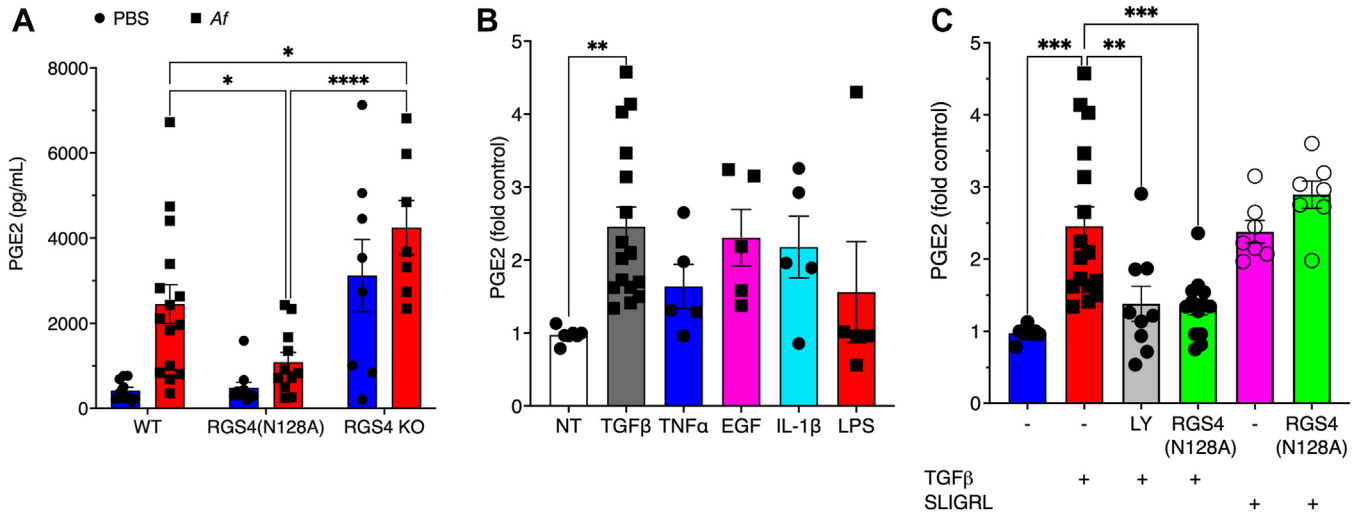

Figure 6. RGS4 regulates PGE2 biosynthesis in lung. *A*, PGE2 levels in BALF. Means ± SEM from n = 7 to 14 mice/group; $^{*}p < 0.04$, $^{****}p < 0.0001$, NA mice *versus* WT, two-way ANOVA test, Tukey's multiple comparisons test. *B* and *C*, PGE2 levels in NHBE cells treated as indicated. *B*, means ± SEM of 7 to 16 biological replicates from two to three independent experiments; $^{**}p = 0.008$ *versus* no treatment (NT), one-way ANOVA test, Dunnett's multiple comparisons test. *C*, $^{**}p = 0.005$, $^{***}p < 0.007$, one-way ANOVA test, Tukey's multiple comparisons test. BALF, bronchoalveolar lavage fluid; NHBE, normal human bronchial epithelial; PGE2,prostaglandin E2; RGS, regulator of G protein signaling.

considered the possibility that it regulates PI3K-dependent PGE2 secretion. To identify potential G protein-independent mediators involved, we stimulated normal human bronchial epithelial (NHBE) cells with several asthma-associated cytokines linked to PGE2 biosynthesis (26–30). Although tumor necrosis factor alpha (TNFα), epidermal growth factor (EGF), IL-1β, or lipopolysaccharide (LPS) had modest or no effects on PGE2 secretion, transforming growth factor beta (TGFβ) significantly increased PGE2 content in NHBE cell supernatants, and this response was strongly inhibited by pretreatment with the PI3K inhibitor LY294002 (Fig. 6, *B* and *C*). To determine the importance of RGS4 GAP activity for PGE2 secretion, we transduced NHBE cells with a tat-GFP-RGS4(N128A) fusion protein (31). Pretreatment of cells with tat-RGS4(N128A) significantly decreased TGFβ-evoked PGE2 secretion in these cells (Fig. 6*C*) but had no effect on the G protein-dependent response to a peptide agonist (SLIGRL) of protease-activated receptor 2.

Mapping the RGS4–PI3K interaction

Although these findings suggested that RGS4 inhibits TGFβ-mediated PGE2 secretion independently of its GAP activity, the mechanism(s) involved remained unclear. Considering our previous findings that RGS4 coimmunoprecipitates specifically with the phosphorylated p85α subunit of PI3K in human ASM cells (17), we hypothesized that it reduces TFGβ-induced PGE2 synthesis by interfering with PI3K activation. To further characterize the RGS4–p85α association, we mixed recombinant 6His-RGS4 (full length and truncated mutants) with recombinant p85α preincubated with Lyn kinase to induce Tyr phosphorylation and collected protein complexes with nickel-coupled agarose beads. Consistent with our previous studies of RGS13 and 16 (15, 16), full-length and N-terminal RGS4 (amino acids [aa] 1–130) but not its C terminus (aa 131–250) bound p-p85α (Fig. 7*A*). Coimmunoprecipitation of GFP-RGS4 and myc-GFP-p85α in transfected HEK293T cells revealed that RGS4 truncations containing aa 1 to 58 and aa 1 to 90 but not the N terminus (aa 1–30) coprecipitated with p85α (Fig. 7*B*). Considering our prior mapping studies of RGS16–p85α interactions (16), these data suggested that aa 30 to 90 in RGS4 mediated its binding to p85α. To pinpoint the specific residues involved, we introduced point substitutions into a region of RGS4 that is highly conserved in R4 RGS proteins (aa 53–62) (Fig. 7*C*) and evaluated binding of cell lysates from transfected HEK293T cells with recombinant 6His-p85α coupled to nickel beads. These studies demonstrated that the E54A and S62A mutations significantly reduced binding to p85α (Fig. 7, *D* and *E*). Likewise, tat GFP-RGS4 (E54A/N128A) and tat GFP-RGS4(S62A/N128A) proteins from transduced HEK293T lysates bound poorly to p85α *in vitro* (Fig. S3).

RGS4 regulates PI3K signaling

Our studies thus far suggested that RGS4 inhibits TGFβ-induced PGE2 secretion in the airways. To determine whether

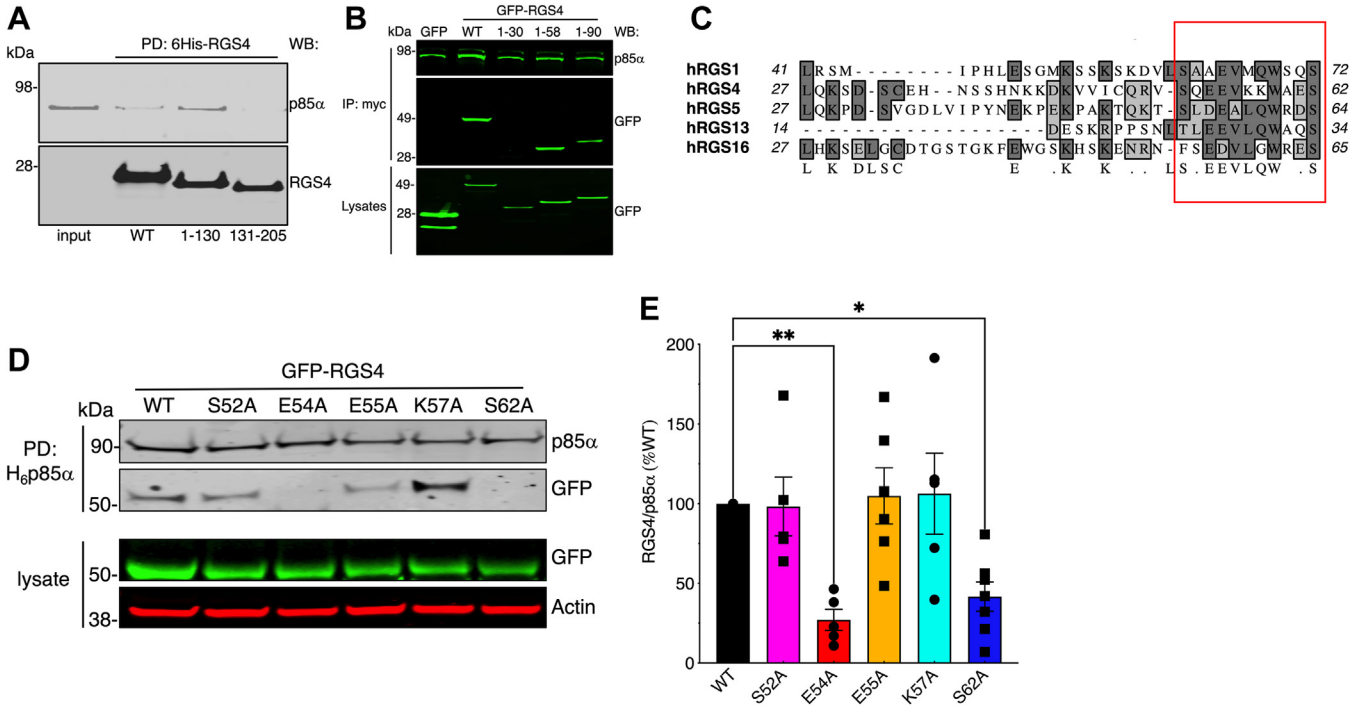

Figure 7. PI3K–RGS4 interactions. *A*, complexes of recombinant p85α pretreated with Lyn kinase and then mixed with 6His-RGS4 were collected with nickel-coated beads. Reactions were immunoblotted as indicated. *B*, lysates from HEK293T cells transfected with plasmids encoding myc-GFP p85α, constitutively active Src(Y529F) and GFP-RGS4 were immunoprecipitated with Myc antibody, and reactions were immunoblotted with GFP. Blots in *A* and *B* represent three similar experiments. *C*, alignment of residues in R4 RGS proteins. *Boxed area* delineates conserved residues previously implicated in RGS13 and RGS16 binding to p85α. *D*, representative blot of 6His-p85α and GFP-RGS4 in lysates of transfected HEK293T cells collected with nickel-coupled agarose and immunoblotted as indicated. GFP-RGS4 expression in total cell lysates is shown in the *lower panel*. *E*, RGS4/p85α band intensities quantified using ImageJ. Means ± SEM from n = 5 to 7 independent experiments; *p = 0.02, **p = 0.007, Kruskal–Wallis ANOVA test, Dunnett's multiple comparisons test. HEK293T, human embryonic kidney 293T cell line; RGS, regulator of G protein signaling.

this occurred through regulation of PI3K, we evaluated the effects of RGS4 overexpression in COS-7 cells on a canonical PI3K signaling pathway (Akt phosphorylation) induced by EGF stimulation. EGF elicited robust Akt phosphorylation at 5 min or 15 min poststimulation. While overexpression of RGS4(N128A) or (E54A/N128A) significantly inhibited this response, expression of RGS4(S62A/N128A) had little to no effect (Fig. 8, *A* and *B*). Likewise, transduction of NHBE cells with N128A or E54A/N128A tat fusion proteins reduced TGFβ-evoked PGE2 production, whereas transduction of the S62A/N128A mutant had no impact (Fig. 8*C*). Because E54A mutant appeared to regulate these processes even more effectively than N128A, these findings suggest that the E54–p85α interaction may negatively regulate the ability of RGS4 to inhibit p85α-dependent functions. In contrast, the S62 residue, which is highly conserved in nearly all R4 RGS proteins (Fig. 7*C*), appears to be critical for RGS4's regulation of PI3K signaling.

PI3K target gene expression in NA mice

An RNA-Seq study done on lung tissues from WT and RGS4 KO mice revealed several relevant PI3K-regulated targets among the 417 genes in naïve mice and 28 genes in allergen-challenged mice that were significantly differentially expressed between these strains (full results in Table S1); top hits in *Af*-challenged mice are shown in Fig. 9*A*. Secondary analysis of these results demonstrated enrichment of genes involved in class I PI3K-dependent processes, including heat shock (32), B-cell receptor (33), epidermal growth factor receptor (34), and Ephrin B (35) signaling pathways (Fig. 9*B*). Among the top differentially regulated genes, *Cdkn1a* encodes the checkpoint protein $p21^{WAF1/Cip1}$, which is regulated by both TGFβ and PI3K signaling (36–38). *Cdkn1a* expression was significantly higher in RGS4 KO mice than in either NA mice or WT controls (Fig. 9*C*). These results provide further evidence of RGS4's regulation of PI3K signaling, which is preserved in NA mice.

Discussion

RGS proteins are expressed in all tissues, and many cell types express closely related paralogs with similar GAP activity profiles on individual Gα subunits *in vitro* (18). A challenge in the field is to determine whether individual RGS proteins have overlapping or redundant physiological functions. Confounding these attempts are results suggesting that RGS proteins also exert control over G protein signaling through interactions with other proteins including GCPRs (39) or downstream G protein effectors such as phospholipase Cβ or adenylyl cyclase (40, 41). Despite these challenges, recent studies done in living systems have established sequence-level differences in individual RGS proteins that are involved in Gα recognition and may confer selective functions (19).

At the organismal level, studies of mice-harboring alleles in *Gnai2* (encoding G148S in Gαi2) that abolish interactions with

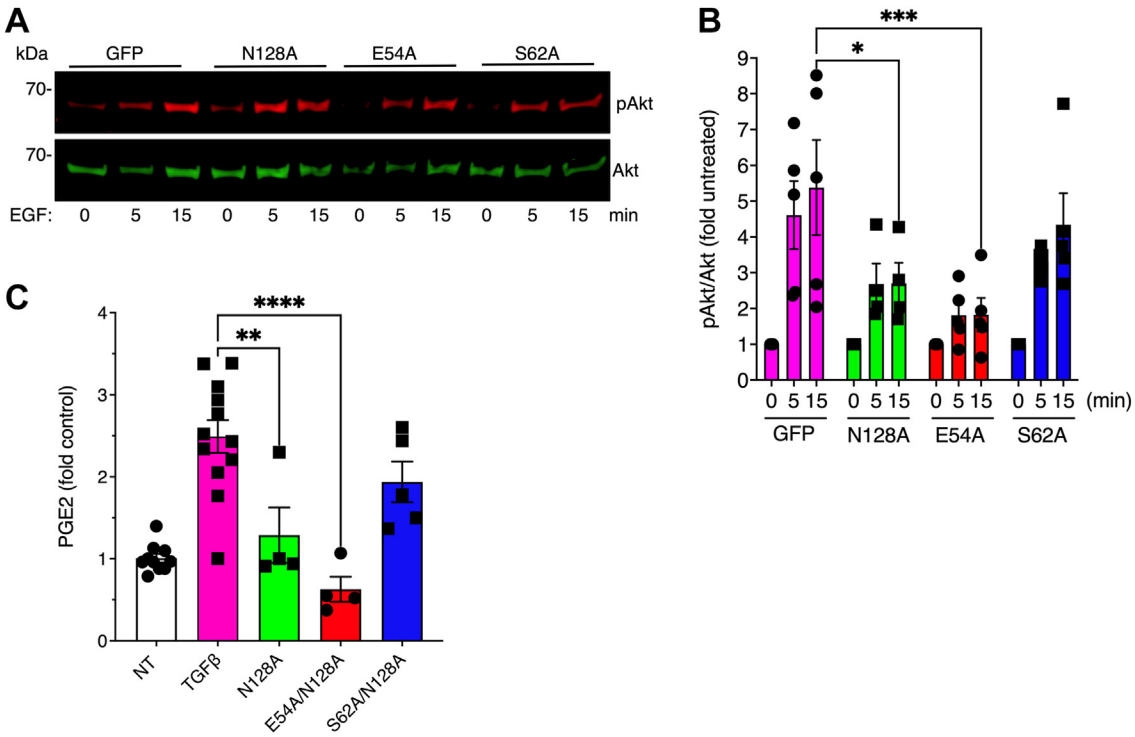

Figure 8. Mechanisms of PI3K regulation by RGS4. *A*, representative blot of phospho- and total Akt in lysates from COS-7 cells transfected with GFP or GFP-RGS4 (WT and mutants) left untreated or stimulated with EGF (30 ng/ml) for the indicated times. *B*, quantification of pAkt/Akt. Means ± SEM from n = 4 to 5 experiments; *p = 0.02, ***p = 0.009 *versus* GFP, two-way ANOVA test, Tukey's multiple comparisons test. *C*, PGE2 levels in NHBE cells treated as indicated. Means ± SEM from 4 to 12 biological replicates from two independent experiments; **p = 0.002, ****$p < 0.0001$ one-way ANOVA test, Tukey's multiple comparisons test. EGF, epidermal growth factor; NHBE, normal human bronchial epithelial; PGE2, prostaglandin E2; RGS, regulator of G protein signaling.

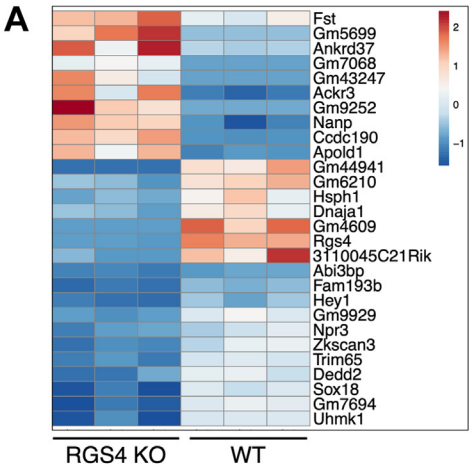

B

Name	p-value
Cellular response to heat stress	1.24E-08
Regulation of HSF1-mediated heat shock response	3.86E-06
Adaptive Immune System	4.69E-06
BCR signaling pathway	1.75E-05
CXCR4-mediated signaling events	5.51E-05
Leukocyte transendothelial migration	5.75E-05
Class I PI3K signaling events mediated by Akt	1.05E-04
Cellular responses to stress	1.15E-04
Innate Immune System	1.82E-04
EGF receptor signaling pathway	2.21E-04
Chemokine signaling pathway	2.75E-04
Cytokine Signaling in Immune system	2.95E-04
Ephrin B reverse signaling	3.19E-04
Inflammation mediated by chemokine and cytokine signaling pathway	4.39E-04
Cytokine-cytokine receptor interaction	4.73E-04
Signaling by Interleukins	4.88E-04
Genes related to PIP3 signaling in cardiac myocytes	8.06E-04
PI3K-Akt signaling pathway	8.69E-04

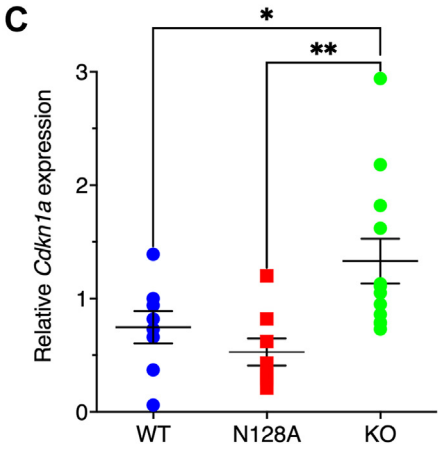

Figure 9. Gene expression patterns in RGS4 KO and N128A mice. *A*, heat map of gene expression patterns in lung tissue from WT and RGS4 KO mice as determined by RNA-Seq (n = 3/group). *B*, enriched pathways in differentially expressed gene sets determined by KEGG, Reactome, Panther analysis, together with Benjamini–Hochberg-corrected *p* values. *C*, relative expression of *Cdkn1a* (normalized by *Actb*) in lung tissue; means ± SEM from n = 8 to 12 mice/group; **p* = 0.04, ***p* = 0.008, one-way ANOVA test, Holm–Sidak multiple comparisons test. KEGG, Kyoto Encyclopedia of Genes and Genomes; RGS, regulator of G protein signaling.

all RGS proteins have revealed important roles for RGS GAP activity on Gαi2 in myocardial injury, opioid tolerance, and growth hormone secretion among others (42, 43). However, studies of these mice do not allow identification of the specific RGS protein involved in these processes. Here, we have shown that NA mice expressing GAP-deficient RGS4 have increased allergen-associated AHR compared with animals completely devoid of RGS4. Our mechanistic studies suggest that RGS4 has distinct GAP-mediated and GAP-independent functions in the lung.

The phenotypic similarities between NA and RGS4 KO mice reveal the importance of RGS4 GAP activity in the pathways involved. Both strains exhibit signs of fatty liver, previously suggested to be a consequence of dysregulated ACh-induced catecholamine secretion in adrenal glands of RGS4 KO mice, which in turn leads to increased circulating free fatty acids (21). Also consistent with the role of RGS4 GAP activity in ACh responses is the finding that airways from NA mice exhibited hypercontraction to muscarinic receptor stimulation *ex vivo*. Reduced *Rgs5* expression in lung tissue from NA mice might also contribute to this phenotype since *Rgs5*−/− mice have spontaneous AHR in the absence of allergic lung inflammation (6). Airway mucus was also increased in allergen-challenged NA mice relative to controls, suggesting that RGS4 GAP activity inhibits GPCR-evoked mucin expression in AECs. These results are consistent with published studies demonstrating that RGS4 dampens $P2Y_2$ receptor–induced *MUC5AC* expression induced by ATP (44).

By contrast, the airway inflammatory milieu in allergen-challenged NA mice differed significantly from either WT or RGS4 KO mice, suggesting GAP-independent functions of RGS4. Levels of allergy-related cytokines were significantly lower in the airways of NA mice than in RGS4 KO mice. We hypothesized previously that increased airway levels of IL-5 and IL-13 in RGS4 KO mice resulted from an expanded innate lymphoid cell type 2 (ILC2) population in lungs; taken together, these findings suggest that RGS4 may influence ILC2 development/expansion through GAP-independent mechanisms (7). Levels of PGE2, an airway mediator with both bronchodilatory and anti-inflammatory actions (45), were significantly lower in NA mice relative to RGS4 KO mice or controls. Since PGE2 inhibits ILC2-mediated cytokine

production (46), these results suggest one potential mechanism for decreased cytokine levels in lungs of RGS4 NA mice.

Our previous studies suggested that increased airway PGE2 is critical to reducing AHR in RGS4 KO mice (7). Although the stimuli for differential PGE2 biosynthesis in NA and RGS4 KO mice are not fully clear, we focused here on TGFβ in light of earlier studies linking it to increased expression of cyclooxygenase 2 (a critical enzyme for PGE2 biosynthesis) through PI3K signaling and the known interaction of RGS4 with PI3K (17, 47). While treatment of NHBE cells with a PI3K inhibitor or GAP-deficient RGS4(N128A) reduced TGFβ-induced PGE2 production, transduction with a RGS4 mutant unable to bind p85α (S62A) had no effect on the response. These results suggest that TGFβ induces PGE2 biosynthesis in part through the PI3K pathway in an RGS4-dependent manner.

The detailed molecular mechanism(s) by which RGS4 modulates TGFβ-evoked PGE2 secretion require further study. Although RGS6 suppresses TGFβ signaling in fibroblasts by interacting with SMAD4 and preventing dimerization with other SMADs, this interaction requires the Gγ-like (GGL) domain of RGS6, which is not present in RGS4 (48). Previously, we demonstrated that RGS16 binds to p85α through its amino-terminal SH2 and inter-SH2 domains, which are critical for its interactions with receptors through adapter proteins such as Gab1 (16). Since RGS16 inhibits p85α–Gab1 interactions, RGS4 might likewise interfere with formation of the complex between the TGFβ type I receptor and p85α (49).

Also consistent with the capacity of RGS4 to regulate PI3K signaling is the finding of differential PI3K target gene expression in the lungs of NA mice relative to the other strains (WT or RGS4 KO), which may contribute to AHR. Increased $p21^{WAF1/Cip1}$ expression is commonly found in ASM from patients with chronic asthma and allergen-challenged mice (50). $p21^{WAF1/Cip1}$ promotes permanent cell cycle arrest (senescence). ASM cell senescence increases ASM mass, a prominent feature of established asthma thought to promote airway obstruction. Senescent ASM cells secrete more cytokines, proteases, growth factors, and extracellular matrix proteins, which may also contribute to airway remodeling (50). Our preliminary findings warrant examination of these parameters in NA mice using models of chronic asthma elicited by long-term and repetitive allergen challenge.

The RGS domain of R4 RGS proteins contains three stretches of highly conserved residues (E82–N88, A123–R134, and K154–S171 in RGS4) that provide essential contributions to GAP activity (18). Although N128 variants have not been detected in humans, ultrarare and predicted LOF variants at critical residues within these regions have been reported in gnomAD (www.gnomad.broadinstitute.org), including Y84H, D130G, R134W, D163N, D163G, and R167H. These findings are compatible with our results showing that RGS4 GAP activity is not essential for survival. Our RGS4 GAP-deficient model provides a new tool to dissect the G protein-dependent and -independent actions of RGS4 on intracellular signaling pathways in asthma and other diseases linked to this RGS protein.

Experimental procedures

Mouse strains

$Rgs4^{-/-}$ mice were generated as described previously (7). Balb/cJ control mice were purchased from The Jackson Laboratories. *Rgs4* (N128A) knockin mouse line was generated using the CRISPR–Cas9 method (51). Briefly, an sgRNA (5′-CTTTGCACTTCAGGTGAACC-3′) designed to cut near the N128 site of mouse *Rgs4* genomic DNA was made by Synthego, and a single-stranded oligonucleotide donor (GCCTCCTC TCTTCAACAGGGCACTAGATCTAATGCAACCTTGGTC TTTGCACTTCAGGTG**GCT**CT**C**GACTCTTGCACCAGAG AGGAGACAAGCCGGAACATGTTACAGCCCACAATAAC CTGTTTTG) was purchased from IDT. The first three bolded deoxyribonucleotides encode the desired mutation, whereas the downstream bolded deoxyribonucleotide encodes a synonymous mutation to prevent off target Cas9 cutting. The sgRNA (20 μg/ml) and donor oligonucleotides (100 μg/ml) were comicroinjected into the cytoplasm of zygotes collected from C57Bl/6N mice (Charles River Laboratories) together with synthetic *Cas9* mRNA (50 μg/ml; TriLink BioTechnologies). Injected embryos were cultured overnight in KSOM medium (MilliporeSigma) in a 37 °C incubator with 6% CO_2. The next day morning, embryos that had reached the two-cell stage of development were implanted into the oviducts of pseudopregnant surrogate mothers (CD1 strain from Charles River Laboratory). Offspring born to the foster mothers were genotyped using PCR (forward primer: CAGCCACTCCTTGTTCATTCC; reverse primer: GGTCAGGTCAAGATAGA ATCG) followed by Sanger sequencing. Founder mice with the desired amino acid change were bred with WT C57BL/6N mice to establish the N128A knockin mouse line. NA mice were subsequently backcrossed onto the Balb/cJ background for four to five generations. All studies were performed in accordance with the institutional guidelines provided by the National Institute of Allergy and Infectious Diseases Animal Use and Care Committee under approved studies (Animal Study Protocols LAD3e and NHLBI protocol H-0125R5).

Reagents, cells, and antibodies

Primary human bronchial epithelial cells were obtained from American Type Culture Collection and cultured in airway epithelial medium (American Type Culture Collection). HEK293T and COS-7 cells were cultured in complete Dulbecco's modified Eagle's medium supplemented with 10% fetal calf serum and antibiotics (ThermoFisher). CCh, MCh, vecuronium, SLIGRL, and LPS were purchased from Sigma. Recombinant EGF, IL-1β, TGFβ, and TNFα were from R&D Systems. Antibodies were purchased from the following sources: RGS4 (catalog no.: ABT17) and β-actin were from Sigma Millipore; p85α (Cell Signaling Technology); and Myc (clone 9E10) and GFP were from Santa Cruz Biotechnology. Recombinant 6His-p85α was purchased from MyBioSource, and 6His-lyn kinase was from Sigma.

Plasmids, recombinant proteins, and transfections

Plasmids encoding active Src(Y529F), myc-GFP p85α were the gift of J. Silvio Gutkind (UC San Diego School of Medicine). HEK293T cells were transfected with plasmids encoding GFP-RGS4 (WT and mutants) and myc-GFP p85α using Lipofectamine 2000 (ThermoFisher). Full-length GFP-RGS4 was subcloned into pTAT-6His-HA (the gift of Stephen Dowdy, University of California, San Diego School of Medicine). Recombinant TAT proteins were expressed in *Escherichia coli* and purified using Ni^{2+}–nitrilotriacetic acid–coupled agarose beads (Roche) as described previously (52). Point mutations were introduced into GFP-RGS4 using the QuikChange XL kit (Agilent Biotechnologies). TAT fusion proteins were added directly to the culture medium (final concentration of 200 nM) 1 h prior to cell stimulation.

6His-RGS4 WT and 6His-Thioredoxin-RGS4 truncation mutants were prepared as described previously (14). All RGS4 constructs were based on the sequence of isoform 2 (NP_005604.1).

RNA isolation and quantitative RT–PCR

RNA was isolated using the RNeasy kit (Qiagen) according to the manufacturer's instructions. Total RNA (500 ng) was reverse transcribed into complementary DNA using SuperScript IV VILO Master Mix (Thermo Fisher) according to the manufacturer's protocol. Quantitative PCR was performed using gene-specific TaqMan probes (ThermoFisher) according to the manufacturer's guidelines. TaqMan probes were as follows: *Rgs2*, Mm00501385_m1; *Rgs4*, Mm00501389_m1; *Rgs5*, Mm00654112_m1; *Actb*, Mm01205647_g1; and *Cdkn1a*, Mm00432448_m1.

Immunoprecipitation/pulldown, immunoblotting, and fluorescence microscopy

Cells were lysed in radioimmunoprecipitation (RIPA) lysis buffer (Sigma) containing protease and phosphatase inhibitors (cOmplete protease inhibitor mixture and PhosSTOP tablets; Roche Applied Science) and sodium orthovanadate (1 μm). Tissues were flash frozen in LN_2 and resuspended in RIPA buffer prior to homogenization with a BeadBlaster 24 homogenizer (Benchmark Scientific). Cell lysates were incubated with 2 μg of mouse monoclonal RGS4 antibody (D-1) (Santa Cruz; catalog no.: sc-398658) and protein A/G-coupled agarose beads for 3 h at 4 °C. Immunoprecipitates were washed three times with RIPA buffer prior to addition of NuPAGE SDS sample buffer (ThermoFisher), boiling at 95 °C for 5 min, and brief centrifugation. Clarified lysates were electrophoresed on 12% NuPAGE Tris–glycine gels and immunoblotted with the indicated antibodies. In pull-down experiments, 6Hisp85α (250 ng; MyBioSource) was incubated with 6His-Lyn (50 ng; Sigma) in buffer containing 60 mM Hepes (pH 7.5), 3 mM $MgCl_2$, 3 mM $MnCl_2$, 1 mM ATP, and 3 mM Na_3VO_4 for 30 min at 30 °C. Phosphorylated 6His-p85α was incubated with lysates from GFP-RGS4-transfected HEK293T cells, and complexes were collected with nickel-coupled agarose beads in binding buffer containing 50 mM Hepes (pH 7.5), 150 mM NaCl, 5 mM $MgCl_2$, 5% glycerol, 0.04% Triton X, and 10 mM imidazole for 1 h at 4 °C. Beads were washed three times with binding buffer prior to addition of SDS sample buffer and immunoblotting. For pulldowns of recombinant proteins, RGS4 WT was cloned into pET15b; truncations (aa 1–130 or 131–205) were cloned into pET-TRXHis6 (Novagen). Proteins were expressed in *E. coli* and purified as aforementioned. Untagged p85α (Jena Bioscience) was incubated with 6His-RGS4 WT or 6His-thioredoxin RGS4 fusion proteins, collected with nickel-coupled agarose, and processed as aforementioned. For visualization of GFP-RGS4 localization, cells were plated into Chamberwell slides for transfection. About 24 h after transfection, cells were fixed with 4% paraformaldehyde in PBS for 10 min at room temperature. Nuclei were counterstained with 4′,6-diamidino-2-phenylindole (Sigma; 1 μg/ml) and examined with a Leica DMI4000B fluorescence microscope.

Complete blood counts

Leukocyte counts and hematological parameters were determined using the Hemavet 950 Multispecies Analyzer (Drew Scientific/Erba Diagnostics).

Allergic airway inflammation model

About 8-12-week-old female mice were sensitized with a mixture of one part alum and one part PBS containing *Af* extract (25 μg protein; HollisterStier Allergy), by i.p. injection on days 0 and 14. Two weeks later, mice were then challenged intranasally with either PBS or *Af* (20 μg) daily for 3 consecutive days. For assessment of lung inflammatory cells, we collected BALF by injection and collection of PBS–1 mM EDTA (1 ml) through a tracheal cannula. Red blood cells were lysed with ACK lysis buffer, and clarified BALF supernatants were frozen and stored at −80 °C. Cell pellets were resuspended in PBS–EDTA counted by hemocytometry and dispersed on glass microscope slides by cytospin.

Diff-Quik-stained slides were used to determine cell composition by microscopy (n = 500 cells/slide). Left lungs were fixed in 10% neutral-buffered formalin for generation of paraffin-embedded sections. Sections were stained with hematoxylin and eosin and PAS. The PAS^+ area of epithelium was quantified using ImageJ (NIH) and divided by the airway diameter to calculate the percentage of positively stained airway.

Lung resistance measurements

About 24 h after the last challenge, mice were anesthetized with a mixture of ketamine (100 mg/kg) and xylazine (10 mg/kg) *via* i.p. injection. Mice tracheas were dissected and cannulated with a 20-gauge catheter. Mice were then paralyzed with vecuronium bromide (200 μg *via* i.p. injection) and mechanically ventilated using the FlexiVent FX1 respirator (SCIREQ). Lung resistance was measured by the pulse oscillometry technique at baseline and after inhalation of increasing doses of MCh.

PGE2 and cytokine measurements

PGE2 levels in BALF and cell culture supernatants were measured by ELISA (Cayman Chemical). NHBE cells were stimulated with TGFβ (5 ng/ml), TNFα (10 ng/ml), EGF (50 ng/ml), IL-1β (1 ng/ml), or LPS (100 ng/ml) for 6 h at 37 °C. Cytokines in BALF supernatants were analyzed using a customized MultiPlex bead array (Bio-Rad) as previously described (7).

Measurement of airway mechanics in PCLS

Mice were euthanized, and the trachea was cannulated with a blunt-end stub adapter secured with a suture. Lungs were inflated with 2% SeaPlaque low melting point temperature agarose in PBS without Ca^{2+} and Mg^{2+} using a syringe. Mice were then placed on ice for 1 h to solidify agarose. The left lobe was excised and embedded in a mold using low melting point agarose. Lung slices (210 μm) were prepared using the Krumdieck Tissue Slicer MD4000 (Alabama Research and Development). They were washed once with serum-free Dulbecco's modified Eagle's medium and incubated overnight at 37 °C in a tissue culture incubator (5% CO_2). Intact slices were anchored by platinum weights containing nylon threads and stimulated with increasing concentration of CCh (10^{-9} to 10^{-4} mol). Images of the airway were taken before and at t = 5 min poststimulation. Images were analyzed using ImageJ, and contraction of the airway was calculated by measuring the luminal area after stimulation as a percentage of the baseline luminal area. Airways not contracting (<10%) in response to agonist were excluded from the analysis.

Statistical analysis

Values are reported as mean ± SEM unless otherwise specified. Normally distributed data were analyzed by t test (two groups) or one- or two-way ANOVA test (multiple groups). For non-normally distributed data, nonparametric Mann–Whitney U test or Kruskal–Wallis tests were used. p Values <0.05 were considered to be significant.

Data and materials availability

All data are available in the main text or supporting information. RNA-Seq results have been deposited into Gene Expression Omnibus (accession no.: GSE242546).

Supporting information—This article contains supporting information (Figs. S1–S3 and Table S1).

Acknowledgments—This work was supported by the Division of Intramural Research, National Institute of Allergy and Infectious Diseases/National Institutes of Health.

Author contributions—K. M. D. conceptualization; K. M. D. methodology; I. V. J., E. C. C., C. L., and K. M. D. investigation; I. V. J., E. C. C., J. B. L., and K. M. D. data curation; K. M. D. writing–original draft; I. V. J., E. C. C., C. L., and J. B. L. writing–review & editing; I. V. J., C. L., and K. M. D. visualization.

Funding and additional information—This work was supported by the National Institutes of Health grant ZIA AI000939-19 (to K. M. D.). The content is solely the responsibility of the authors and does not necessarily represent the official views of the National Institutes of Health. The content of this publication neither does necessarily reflect the views or policies of the Department of Health and Human Services nor does the mention of trade names, commercial products, or organizations imply endorsement by the US government.

Conflict of interest—The authors declare that they have no conflicts of interest with the contents of this article.

Abbreviations—The abbreviations used are: ACh, acetylcholine; AEC, airway epithelial cell; AHR, airway hyper-responsiveness; ASM, airway smooth muscle; BALF, bronchoalveolar lavage fluid; CCh, carbachol; EGF, epidermal growth factor; GAP, GTPase-activating protein; GPCR, G protein-coupled receptor; HEK293T, human embryonic kidney 293T cell line; IL, interleukin; ILC2, innate lymphoid cell type 2; LPS, lipopolysaccharide; MCh, methacholine; NHBE, normal human bronchial epithelial; PAS, periodic acid Schiff; PCLS, precision cut lung slice; PGE2, prostaglandin E2; RGS, regulator of G protein signaling; RIPA, radioimmunoprecipitation; sgRNA, single guide RNA; TGFβ, transforming growth factor beta; TNFα, tumor necrosis factor alpha.

References

1. Spahn, J. D., Brightling, C. E., O'Byrne, P. M., Simpson, L. J., Molfino, N. A., Ambrose, C. S., *et al.* (2023) Effect of biologic therapies on airway hyperresponsiveness and allergic response: a systematic literature review. *J. Asthma Allergy* **16**, 755–774
2. Ji, T., and Li, H. (2023) T-helper cells and their cytokines in pathogenesis and treatment of asthma. *Front Immunol.* **14**, 1149203
3. Hsieh, A., Assadinia, N., and Hackett, T. L. (2023) Airway remodeling heterogeneity in asthma and its relationship to disease outcomes. *Front Physiol.* **14**, 1113100
4. Fuentes, N., McCullough, M., Panettieri, R. A., Jr., and Druey, K. M. (2021) RGS proteins, GRKs, and beta-arrestins modulate G protein-mediated signaling pathways in asthma. *Pharmacol. Ther.* **223**, 107818
5. George, T., Bell, M., Chakraborty, M., Siderovski, D. P., Giembycz, M. A., and Newton, R. (2017) Protective roles for RGS2 in a mouse model of house dust mite-induced airway inflammation. *PLoS One* **12**, e0170269
6. Balenga, N. A., Jester, W., Jiang, M., Panettieri, R. A., Jr., and Druey, K. M. (2014) Loss of regulator of G protein signaling 5 promotes airway hyperresponsiveness in the absence of allergic inflammation. *J. Allergy Clin. Immunol.* **134**, 451–459
7. Wong, G. S., Redes, J. L., Balenga, N., McCullough, M., Fuentes, N., Gokhale, A., *et al.* (2020) RGS4 promotes allergen- and aspirin-associated airway hyperresponsiveness by inhibiting PGE2 biosynthesis. *J. Allergy Clin. Immunol.* **146**, 1152–1164.e13
8. Cardet, J. C., Kim, D., Bleecker, E. R., Casale, T. B., Israel, E., Mauger, D., *et al.* (2022) Clinical and molecular implications of RGS2 promoter genetic variation in severe asthma. *J. Allergy Clin. Immunol.* **150**, 721–726.e1
9. McNeill, S. M., and Zhao, P. (2023) The roles of RGS proteins in cardiometabolic disease. *Br. J. Pharmacol.* https://doi.org/10.1111/bph.16076
10. Li, L., Xu, Q., and Tang, C. (2023) RGS proteins and their roles in cancer: friend or foe? *Cancer Cell Int.* **23**, 81
11. Montanez-Miranda, C., Bramlett, S. N., and Hepler, J. R. (2023) RGS14 expression in CA2 hippocampus, amygdala, and basal ganglia: implications for human brain physiology and disease. *Hippocampus* **33**, 166–181
12. Popov, S. G., Krishna, U. M., Falck, J. R., and Wilkie, T. M. (2000) Ca2+/Calmodulin reverses phosphatidylinositol 3,4, 5-trisphosphate-dependent

inhibition of regulators of G protein-signaling GTPase-activating protein activity. *J. Biol. Chem.* **275**, 18962–18968
13. Thaminy, S., Auerbach, D., Arnoldo, A., and Stagljar, I. (2003) Identification of novel ErbB3-interacting factors using the split-ubiquitin membrane yeast two-hybrid system. *Genome Res.* **13**, 1744–1753
14. Sullivan, B. M., Harrison-Lavoie, K. J., Marshansky, V., Lin, H. Y., Kehrl, J. H., Ausiello, D. A., *et al.* (2000) RGS4 and RGS2 bind coatomer and inhibit COPI association with Golgi membranes and intracellular transport. *Mol. Biol. Cell* **11**, 3155–3168
15. Bansal, G., Xie, Z., Rao, S., Nocka, K. H., and Druey, K. M. (2008) Suppression of immunoglobulin E-mediated allergic responses by regulator of G protein signaling 13. *Nat. Immunol.* **9**, 73–80
16. Liang, G., Bansal, G., Xie, Z., and Druey, K. M. (2009) RGS16 inhibits breast cancer cell growth by mitigating phosphatidylinositol 3-kinase signaling. *J. Biol. Chem.* **284**, 21719–21727
17. Damera, G., Druey, K. M., Cooper, P. R., Krymskaya, V. P., Soberman, R. J., Amrani, Y., *et al.* (2012) An RGS4-mediated phenotypic switch of bronchial smooth muscle cells promotes fixed airway obstruction in asthma. *PLoS One* **7**, e28504
18. Asli, A., Higazy-Mreih, S., Avital-Shacham, M., and Kosloff, M. (2021) Residue-level determinants of RGS R4 subfamily GAP activity and specificity towards the G(i) subfamily Cell. *Mol. Life Sci.* **78**, 6305–6318
19. Masuho, I., Balaji, S., Muntean, B. S., Skamangas, N. K., Chavali, S., Tesmer, J. J. G., *et al.* (2020) A global map of G protein signaling regulation by RGS proteins. *Cell* **183**, 503–521.e9
20. Asli, A., Sadiya, I., Avital-Shacham, M., and Kosloff, M. (2018) "Disruptor" residues in the regulator of G protein signaling (RGS) R12 subfamily attenuate the inactivation of Galpha subunits. *Sci. Signal* **11**, eaan3677
21. Iankova, I., Chavey, C., Clape, C., Colomer, C., Guerineau, N. C., Grillet, N., *et al.* (2008) Regulator of G protein signaling-4 controls fatty acid and glucose homeostasis. *Endocrinology* **149**, 5706–5712
22. Denning, D. W., and Pfavayi, L. T. (2023) Poorly controlled asthma - easy wins and future prospects for addressing fungal allergy. *Allergol. Int.* **72**, 493–506
23. Devos, F. C., Maaske, A., Robichaud, A., Pollaris, L., Seys, S., Lopez, C. A., *et al.* (2017) Forced expiration measurements in mouse models of obstructive and restrictive lung diseases. *Respir. Res.* **18**, 123
24. Kimura, Y., Shinoda, M., Shinkai, M., and Kaneko, T. (2023) Solithromycin inhibits IL-13-induced goblet cell hyperplasia and MUC5AC, CLCA1, and ANO1 in human bronchial epithelial cells. *PeerJ* **11**, e14695
25. Canonica, G. W., Varricchi, G., Paoletti, G., Heffler, E., and Virchow, J. C. (2023) Advancing precision medicine in asthma: evolution of treatment outcomes. *J. Allergy Clin. Immunol.* **152**, 835–840
26. Vo, B. T., Morton, D., Jr., Komaragiri, S., Millena, A. C., Leath, C., and Khan, S. A. (2013) TGF-beta effects on prostate cancer cell migration and invasion are mediated by PGE2 through activation of PI3K/AKT/mTOR pathway. *Endocrinology* **154**, 1768–1779
27. Casey, M. L., Mitchell, M. D., and MacDonald, P. C. (1987) Epidermal growth factor-stimulated prostaglandin E2 production in human amnion cells: specificity and nonesterified arachidonic acid dependency. *Mol. Cell Endocrinol.* **53**, 169–176
28. Nakao, S., Ogtata, Y., Shimizu, E., Yamazaki, M., Furuyama, S., and Sugiya, H. (2002) Tumor necrosis factor alpha (TNF-alpha)-induced prostaglandin E2 release is mediated by the activation of cyclooxygenase-2 (COX-2) transcription via NFkappaB in human gingival fibroblasts. *Mol. Cell Biochem.* **238**, 11–18
29. Molina-Holgado, E., Ortiz, S., Molina-Holgado, F., and Guaza, C. (2000) Induction of COX-2 and PGE(2) biosynthesis by IL-1beta is mediated by PKC and mitogen-activated protein kinases in murine astrocytes. *Br. J. Pharmacol.* **131**, 152–159
30. Lin, C. Y., Wang, W. H., Chen, S. H., Chang, Y. W., Hung, L. C., Chen, C. Y., *et al.* (2017) Lipopolysaccharide-induced nitric oxide, prostaglandin E2, and cytokine production of mouse and human macrophages are suppressed by pheophytin-b. *Int. J. Mol. Sci.* **18**, 2637
31. Chan, E. C., Ren, C., Xie, Z., Jude, J., Barker, T., Koziol-White, C. A., *et al.* (2018) Regulator of G protein signaling 5 restricts neutrophil chemotaxis and trafficking. *J. Biol. Chem.* **293**, 12690–12702
32. Ye, C., Huang, C., Zou, M., Hu, Y., Luo, L., Wei, Y., *et al.* (2019) The role of secreted Hsp90alpha in HDM-induced asthmatic airway epithelial barrier dysfunction. *BMC Pulm. Med.* **19**, 218
33. Iwata, S., Hajime Sumikawa, M., and Tanaka, Y. (2023) B cell activation via immunometabolism in systemic lupus erythematosus. *Front Immunol.* **14**, 1155421
34. Niu, Y., Fu, X., Lin, Q., Liang, H., Luo, X., Zuo, S., *et al.* (2023) Epidermal growth factor receptor promotes infectious spleen and kidney necrosis virus invasion via PI3K-Akt signaling pathway. *J. Gen. Virol.* **104**. https://doi.org/10.1099/jgv.0.001882
35. Guan, X. H., Lu, X. F., Zhang, H. X., Wu, J. R., Yuan, Y., Bao, Q., *et al.* (2010) Phosphatidylinositol 3-kinase mediates pain behaviors induced by activation of peripheral ephrinBs/EphBs signaling in mice. *Pharmacol. Biochem. Behav.* **95**, 315–324
36. Guo, Q., Xiong, Y., Song, Y., Hua, K., and Gao, S. (2019) ARHGAP17 suppresses tumor progression and up-regulates P21 and P27 expression via inhibiting PI3K/AKT signaling pathway in cervical cancer. *Gene* **692**, 9–16
37. Hu, Z., Long, T., Ma, Y., Zhu, J., Gao, L., Zhong, Y., *et al.* (2020) Downregulation of GLYR1 contributes to microsatellite instability colorectal cancer by targeting p21 via the p38MAPK and PI3K/AKT pathways. *J. Exp. Clin. Cancer Res.* **39**, 76
38. Yamada, Z., Nishio, J., Motomura, K., Mizutani, S., Yamada, S., Mikami, T., *et al.* (2022) Senescence of alveolar epithelial cells impacts initiation and chronic phases of murine fibrosing interstitial lung disease. *Front Immunol.* **13**, 935114
39. Kim, Y., and Ghil, S. (2020) Regulators of G-protein signaling, RGS2 and RGS4, inhibit protease-activated receptor 4-mediated signaling by forming a complex with the receptor and Galpha in live cells Cell. *Commun. Signal* **18**, 86
40. McNabb, H. J., Zhang, Q., and Sjogren, B. (2020) Emerging roles for regulator of G protein signaling 2 in (Patho)physiology. *Mol. Pharmacol.* **98**, 751–760
41. Abramow-Newerly, M., Roy, A. A., Nunn, C., and Chidiac, P. (2006) RGS proteins have a signalling complex: interactions between RGS proteins and GPCRs, effectors, and auxiliary proteins. *Cell Signal* **18**, 579–591
42. Neubig, R. R. (2015) RGS-insensitive G proteins as in vivo probes of RGS function. *Prog. Mol. Biol. Transl Sci.* **133**, 13–30
43. Omouessi, S. T., Leipprandt, J. R., Akoume, M. Y., Charbeneau, R., Wade, S., and Neubig, R. R. (2021) Mice with an RGS-insensitive Galpha(i2) protein show growth hormone axis dysfunction. *Mol. Cell Endocrinol.* **521**, 111098
44. Song, K. S., Kim, H. J., Kim, K., Lee, J. G., and Yoon, J. H. (2009) Regulator of G-protein signaling 4 suppresses LPS-induced MUC5AC overproduction in the airway. *Am. J. Respir. Cell Mol Biol.* **41**, 40–49
45. Cebulla, D., van Geffen, C., and Kolahian, S. (2023) The role of PGE2 and EP receptors on lung's immune and structural cells; possibilities for future asthma therapy. *Pharmacol. Ther.* **241**, 108313
46. Robb, C. T., Zhou, Y., Felton, J. M., Zhang, B., Goepp, M., Jheeta, P., *et al.* (2023) Metabolic regulation by prostaglandin E(2) impairs lung group 2 innate lymphoid cell responses. *Allergy* **78**, 714–730
47. Rodriguez-Barbero, A., Dorado, F., Velasco, S., Pandiella, A., Banas, B., and Lopez-Novoa, J. M. (2006) TGF-beta1 induces COX-2 expression and PGE2 synthesis through MAPK and PI3K pathways in human mesangial cells. *Kidney Int.* **70**, 901–909
48. Wang, Z., Chen, J., Wang, S., Sun, Z., Lei, Z., Zhang, H. T., *et al.* (2022) RGS6 suppresses TGF-beta-induced epithelial-mesenchymal transition in non-small cell lung cancers via a novel mechanism dependent on its interaction with SMAD4. *Cell Death Dis.* **13**, 656

49. Hamidi, A., Song, J., Thakur, N., Itoh, S., Marcusson, A., Bergh, A., *et al.* (2017) TGF-beta promotes PI3K-AKT signaling and prostate cancer cell migration through the TRAF6-mediated ubiquitylation of p85alpha. *Sci. Signal* **10**, eaal4186
50. Wan, R., Srikaram, P., Guntupalli, V., Hu, C., Chen, Q., and Gao, P. (2023) Cellular senescence in asthma: from pathogenesis to therapeutic challenges. *EBioMedicine* **94**, 104717
51. Wang, H., Yang, H., Shivalila, C. S., Dawlaty, M. M., Cheng, A. W., Zhang, F., *et al.* (2013) One-step generation of mice carrying mutations in multiple genes by CRISPR/Cas-mediated genome engineering. *Cell* **153**, 910–918
52. Nagahara, H., Vocero-Akbani, A. M., Snyder, E. L., Ho, A., Latham, D. G., Lissy, N. A., *et al.* (1998) Transduction of full-length TAT fusion proteins into mammalian cells: TAT-p27Kip1 induces cell migration. *Nat. Med.* **4**, 1449–1452